PCCP

# Model Systems for Screening and Investigation of Lithium Metal Electrode Chemistry and Dendrite Formation

| | |
|---|---|
| Journal: | *Physical Chemistry Chemical Physics* |
| Manuscript ID | CP-ART-11-2019-006020.R1 |
| Article Type: | Paper |
| Date Submitted by the Author: | 09-Dec-2019 |
| Complete List of Authors: | Kamphaus, Ethan; Texas A and M University College Station, Chemical Engineering<br>Hight, Karoline; Texas A and M University College Station, Chemical Engineering<br>Dermott, Micah; Texas A and M University College Station, Chemical Engineering<br>Balbuena, Perla; Texas AandM University, Chemical Engineering |
| | |

SCHOLARONE™
Manuscripts

# Model Systems for Screening and Investigation of Lithium Metal Electrode Chemistry and Dendrite Formation

Ethan P. Kamphaus, Karoline Hight, Micah Dermott, Perla B. Balbuena*
Department of Chemical Engineering, Texas A&M University, College Station, TX, 77843
*e-mail: balbuena@tamu.edu

## Abstract

The use of lithium metal as an electrode for electrochemical energy storage will provide a significant impact on practical energy storage technology. Unfortunately, the use of lithium metal is plagued with challenging chemical problems. Specifically, the formation of a solid electrolyte interphase layer and the nucleation and growth of lithium dendrites, both must be addressed and controlled in order to achieve a practically useable pure lithium metal electrode. Currently sophisticated experimental techniques and computationally expensive simulations are being used to probe these problems but these methods are arduous and time consuming which delays timely evaluation and insight into the rapidly changing field of advanced energy storage. Here, we report the use of DFT simulations of lithium nanoclusters to investigate and explore lithium metal chemistry with inexpensive computational methods to gain greater insight into electrochemical reductions and the nucleation and growth of dendrites. DME, LiTFSI, and LiFSI reduction energetics and structures with electrode effects from lithium metal are reported providing better physical description of the absolute reduction potential characterization. The electronic structure of the lithium nanoclusters were used to investigate the nucleation and growth of lithium dendrites from an *ab-initio* perspective. The results demonstrate that kinetic processes have more control over non uniform growth than thermodynamic processes. Based on this information, a non *ab-initio* model was created in Matlab that shows the initial stages of dendrite nucleation considering approximately 2000 atoms.

## Introduction

Given the increasing demands for personal electronics, off grid energy storage and green transportation, battery research and development has been and continues being a very active research field. The complex interconnected nature of the electrochemical systems involved with a long-lasting high-energy density battery presents a challenging interdisciplinary science and engineering problem. Currently the most popular high-performance battery in use is the lithium ion battery. With a specific energy of 250 Wh kg$^{-1}$. the lithium ion battery has been adopted heavily in many different technologies[1]. There is much active research focusing on improving the lithium ion battery further by exploring new materials, electrolytes and clever design strategies. Improvements to materials could change aspects of the battery chemistry, which will affect the overall performance and operation of the system. Unfortunately, many of these types of

improvements will be incremental which do not meet the demands of modern technology. In order to greatly increase the energy storage capabilities of lithium batteries, different materials and chemistries are required. One example of this is to use a lithium metal electrode to replace the lithium graphite electrodes that are currently used. Lithium metal has a high theoretical specific capacity (3,860 mAh g$^{-1}$ )[1] and is required by Lithium sulfur and Lithium air batteries which have specific energies of 2600 Wh kg$^{-1}$ and 3500 Wh kg$^{-1}$ respectively[2, 3].

Lithium metal is highly difficult to incorporate into a battery without causing issues that must be solved before practical application. The extreme reactivity of lithium creates the formation of the solid electrolyte interphase (SEI) layer when exposed to electrolyte[4]. Depending on many factors such as the chemistry and stability of the electrolyte, surface chemistry and structure of the electrode, the SEI can have poor mechanical and electrical properties that make the SEI unstable and challenging to work with[5-8]. The SEI has been the focus of intense study for multiple decades attempting to glean an understanding and control the many complicated chemical processes that govern SEI formation and cycling performance[9-12]. Another poor aspect of using lithium metal is the formation and growth of lithium metal dendrites[13]. These lithium spike-like structures introduce significant safety issues since they can short circuit the battery by connecting electrodes in addition to worse electrochemical performance[14]. In order to harness the energy storage characteristics of lithium metal, these problems must be solved.

There are certain system characteristics that are especially hard to determine experimentally. One example of this is determining the pure reduction or oxidation potentials of specific chemical species[15]. There are ways to determine these potentials from some metals easily, but an entire electrochemical system must be constructed in order to take the measurement. This presents a challenge for chemicals that are not in solid state, for instance different components of the electrolyte like lithium salts. Salts such as LiTFSI or LiPF$_6$ are very important to battery operation and performance but determining an absolute redox potential for these compounds is not trivial. This presents a significant issue especially for exploring new battery chemistries which would introduce new lithium salts and electrolytes. Other important characteristics are connected to chemical and structural changes on a fundamental scale. Currently it takes incredibly precise, complicated and expensive experimental methods to determine the atomic structure of materials especially reduction on a nanoscale or lithium dendrite nucleation[16-19]. Though difficult experimentally, determining reductions, atomic structures and other characteristics can be done with relative ease computationally.

The formation and nucleation of the SEI is particularly important since that can govern the rest of the growth of the SEI and properties. Computational studies have been used to explore the reductions of the electrolyte at an electronic scale and other important processes[20-22]. Cutting edge experimental techniques have been reported recently to also investigate these reactions with molecular level precision[23]. Even with these studies and others, additional understanding is still required. Every time a new electrolyte is reported, this will affect the SEI requiring careful experiments to understand the impact. This provides an opportunity for simulations to assist with

screening and high throughput exploration of chemistries that will prove essential to understanding and controlling of the SEI. The same applies to lithium dendrites. Though they have been the topic of much study, most research has focused on mitigation methods such as separators, protective layers, and additives [13, 24-26]. Unfortunately, the underlying fundamentals of the reasons why lithium grows in that nature are still not entirely known leaving an important research gap that computational simulations can help explore.

Naturally, computational approaches are not without their own faults. Computational simulations allow one to construct ideal scenarios not all of which can be translated into realizable experiments. It is possible to create models that are not representative of a real physical system giving results that are not relevant. As long as thought and care are given to the design of computational models, this can be avoided. Another issue with much simulation and modeling work is that they take a large amount of computational power and resources. There are many examples of simulations especially within the sub field of ab-initio modeling that take much longer than most experiments. Although the information provided by these investigations is highly valuable, these methods provide less potential for quickly screening and evaluating new chemistries to help developing next generation batteries. Due to the wide variety of computational tools available, other models and simulations can be created to accomplish this task.

We report model systems and a methodology for exploring and investigating lithium battery chemistries. Multiple models for determining reduction energies and structures for relevant chemical species were explored and we present a new perspective of lithium reduction, and lithium dendrite nucleation and growth. These models provide a basis for further screening in order to parse the many different potential battery chemistries.

*Methodology*

The quantum chemistry models and simulations were completed with Gaussian09[27] for the calculations themselves and GaussView 6[28] for the creation and visualization of the different models. Density functional theory (DFT) was used for solving the time independent Schrodinger equation due to its relative computational ease and capturing of dynamic electron correlation. Throughout all the simulations used, B3PW91[29] was selected as the hybrid exchange-correlation functional. A hybrid functional was used since they have an exact description of exchange forces that conventional DFT does not. B3PW91 is a popular method and has been used for a wide variety of different systems including LiFSI and LiTFSI[30]. Two different basis sets were used to describe the shape of the molecular orbitals for the models. For all Li cluster sizes under 10 atoms, aug-cc-pvtz[31] was used as the basis set. This triple zeta basis set contains dispersion and polarization while also being considered a large basis set. Since this basis set is large, as the size of the lithium clusters increased this basis set became too challenging for the program to run. For lithium cluster sizes containing 10 atoms or more, 6-311++G(d,p)[32, 33] was used. This is a split-valence double zeta basis set containing diffuse and polarization functions which is not as large as aug-cc-pvtz but still contains important characteristics needed for a good chemical description. For

all simulations, geometry optimizations were carried out to obtain ground state structures. Frequency calculations were also used to determine the free energies and thermochemical properties based on the minimum energy structure. Charge densities, electrostatic potentials and other information was obtained from the optimized simulations and visualized in GaussView. All of the simulations reported in this work use an implicit solvent field representing 1,2-Dimethoxyethane (DME) in order to approximate liquid phase results. This is implemented via the IEFPCM[34, 35] within the self-consistent reactive field methodology. THF was chosen as the model solvent for this method but the dielectric constant was changed to 7.2 to represent DME.

In order to investigate longer time and distance scales such as dendrite formation, a lower level of theory must be used. We developed a program based on the electrostatic potentials of lithium nanoclusters evaluated from first principles simulations so that the basis behind the new program is still fundamental. The electrostatic potentials are used to determine the most preferred routes/locations where the cations can be landing when migrating toward the Li metal clusters. The main objective of this program is to observe if cation deposition guided by the electrostatic potentials simulations can nucleate dendrites and provide a more fundamental understanding of the factors that govern dendrite nucleation, formation and growth. The lithium dendrite growth program was created in Matlab 2018b[36]. The algorithm for the code can be described by the flowchart shown below (Scheme 1). The initial structure used for the spherical geometries was a triangle matching the geometry of the $Li_3$ optimized neutral cluster. For the electrode geometries, a square initial configuration was used. In order to only adding atoms to the available surface, the Matlab function boundary was used to create the surface. This built-in function gives a 3D boundary around the points that are fed into the program with a factor that tailors the "roughness" of the surface created. A parameter of 0.8 was used for all of the simulations reported here. This value was selected to minimize the amount of internal surfaces created. If the value is too high, there will be a large number of internal surfaces, which will greatly slow the program down due to being non-viable addition locations. After the surface is created, a random point on this surface is selected. Then the program checks to see if the selected point is too close to one of the lithium atoms. If it's not too close, then the addition is valid and incorporated into the cluster. This is looped until the cluster achieves the predefined desired size.
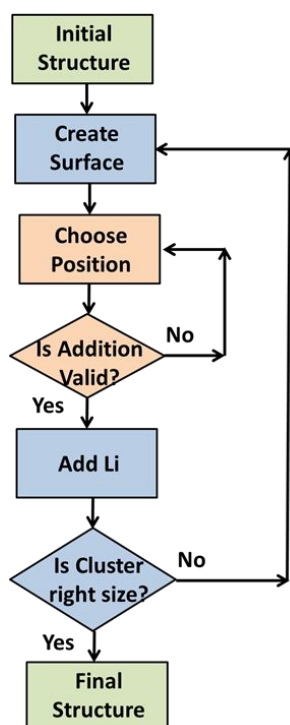
**Scheme 1**: Flowchart for description of dendrite growth algorithm.

## *Results and Discussion*

### Reduction of Electrolyte Species in contact with Li Nanoclusters

One of the most fundamental and important characteristics of a battery chemistry and performance is the reduction and oxidation potentials of the different chemical species present in the battery. Since batteries function by electrochemical reactions, the thermodynamics of those reactions is critical. This is not a new topic of computational chemistry focus and research, but is an important topic that still needs additional study. Usually reduction calculations of a specific chemical only involve one molecule and are done entirely in implicit solvent. The use of an implicit solvent helps estimate the effects of a solvation field (i.e. the bulk electrolyte). This approach is useful but doesn't have any of the finer atomic effects of using actual solvent molecules (explicit solvent). It has been noted in previous research that the combination of explicit solvent molecules with implicit solvation, also known as cluster-continuum solvation, improves the accuracy of results. These sorts of multi molecule effects will change the reduction energies and represent a more realistic system for solvent and non-solvent molecules. Another important factor to consider for reduction calculations is that currently all the reduction calculations have been carried out by simply comparing a neutral system to a system with an added electron. This is what a reduction is in a theoretical sense, but this "pure" reduction potential is perhaps not as useful as one with more factors accounted for. To measure a reduction potential experimentally, one would build an electrochemical cell and polarize and electrode measuring the current. This is essentially injecting

electrons into the system like adding an electron to a molecule in our simulations. The difference lies in the presence of an electrode. An electrode is not required to determine a reduction potential computationally, but electrodes are important to the overall electrochemical process. We can represent an electrode and estimate its effects by using metal clusters. In many cases, the properties of the electrode that we are interested in do not require a high computational expense, such as that involved in traditional periodic boundary conditions calculations. With smaller Li nanoclusters, we can investigate and explore the properties and behavior of lithium metal anode chemistry and use these models to increase the physicality of reduction calculations.

***Li cluster structures.*** Hu et al. reported structures of Li nanoclusters from size $Li_3$ to $Li_{20}$ in solution using highly accurate computational methods[37]. Their study focused on Li nanoclusters for the purposes of spectroscopic analysis and detection but their data gives a starting point for the investigation of Li  metal anodes. The authors determined these structures based on the lowest energy configurations for each cluster size. In the conditions of the simulation, given enough time to reach equilibrium, these will be the thermodynamically expected stable structures. We used the structures from this work to create similar models but with a lower level of accuracy (B3PW91 vs CCSD). The methods used in the original report are too computationally intensive to run further calculations and investigation. The structures from our lower level of theory are shown in Figure 1. The corresponding electron densities can be found in Figure S5.
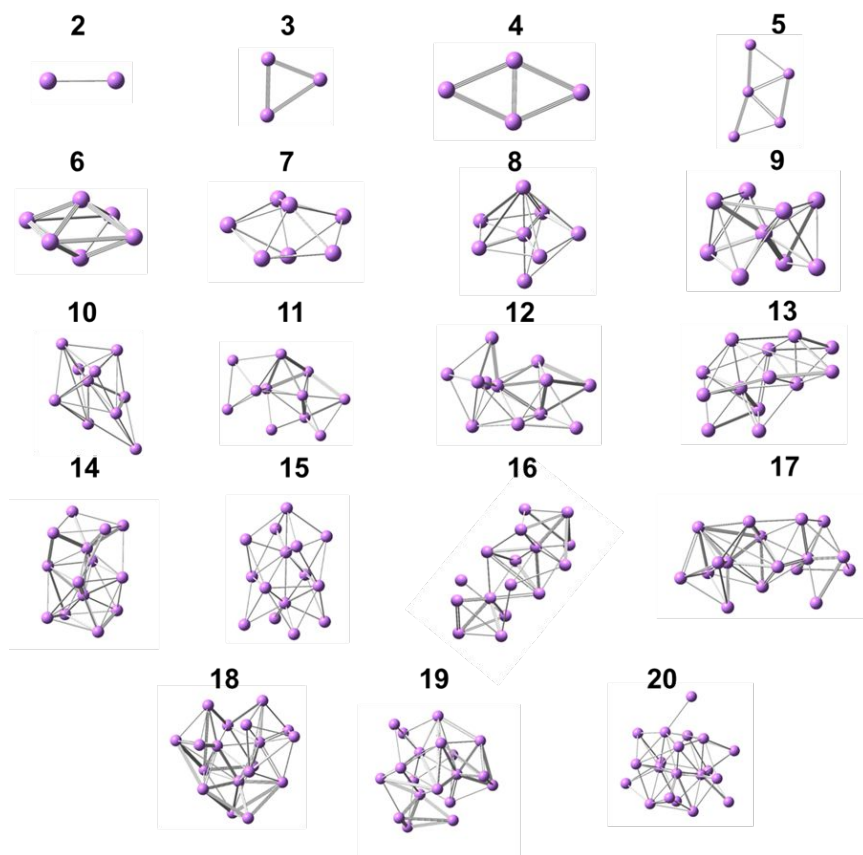
**Figure 1**: Optimized Li nanocluster structures for sizes ($Li_x$, $2 \leq x \leq 20$)

The lithium nanoclusters calculated at a lower level of theory have similar geometries to the more accurate calculations and we are able to determine free energies, electron density, and other important properties. One traditional characterization technique used in first principles modeling is partial charge or population analysis. In a quantum chemistry calculation, the program solves for the electron density, which can be difficult to visualize. Partial charge analysis is the partitioning of the electron density onto atoms. The electron density in this form is more tangible and approachable though it has less resolution than the electron density itself. Lithium clusters or the metal itself have a unique electron density that contains the presence of "ghost" atoms which are the buildup of electron density at locations not centered on a nucleus.[38, 39] The presence of ghost atoms makes the more common partial charge techniques falter. It has been well documented that Bader charge analysis is not dependable in application to lithium metal systems. Though the Bader charge[40] method is a useful method for most systems, it may not be applicable to lithium metal systems.

***Evaluation of atomic charges.*** Gaussian 09 has several different types of available population analysis, which provided an opportunity to test and compare how each one partitions the unique lithium cluster electron density. Figure 2 contains the results for the clusters in comparison. Bader charges seem to suffer the most from variability. In a large number of clusters, Bader charges predicts very high and low partial charges which is indicative of poor partitioning of the electron density. Other charge schemes that are implementable in Gaussian were investigated as alternatives. Natural bond order (NBO)[40] uses configuration interaction based orbital schemes to localize the charge density, HLY involves the regression of the electrostatic potential to fit the charges[41], atomic polarization tensor (APT)[42] involves the partitioning of the polarization tensor based on mathematical rules and Mulliken uses a 50/50 division scheme between atoms. Mulliken is the least sophisticated method out of all the tested schemes but it gives quite reasonable partial charges. APT also provides reasonable partial charges for the Li atoms and it uses a more physical method to partition the electron density which gives similar values to Mulliken analysis. As the size of the clusters increase, the lithium atoms move from being all on the surface of the cluster to having one or two atoms inside of the cluster. This change can be observed in the partial charge graphs by large negative partial charges on particular atoms. This is due to the multidirectional nature of metallic bonds. Methods like Bader charges and HLY show very high partial charges for those atoms. In the case of $Li_8$, the internal atom is assigned ~7 e of charge for these two methods. This goes against chemical intuition and reasonability. APT and Mulliken always provide fair numbers for the partial charges while NBO has variability based on the cluster. Between Mulliken and APT, APT has a more fundamental theory behind it because of the partitioning of the polarization tensor, which is based on the derivatives of the energy in the simulation. On the other hand, Mulliken, is a non-sophisticated method that divides the electron density equally between the atoms. Based on the physicality and reasonability of the partial charge scheme, we believe APT to be the most reliable for these systems. This analysis provides a better

tool for examining partial charges in Li metal based systems which should be incorporated into other computational studies.
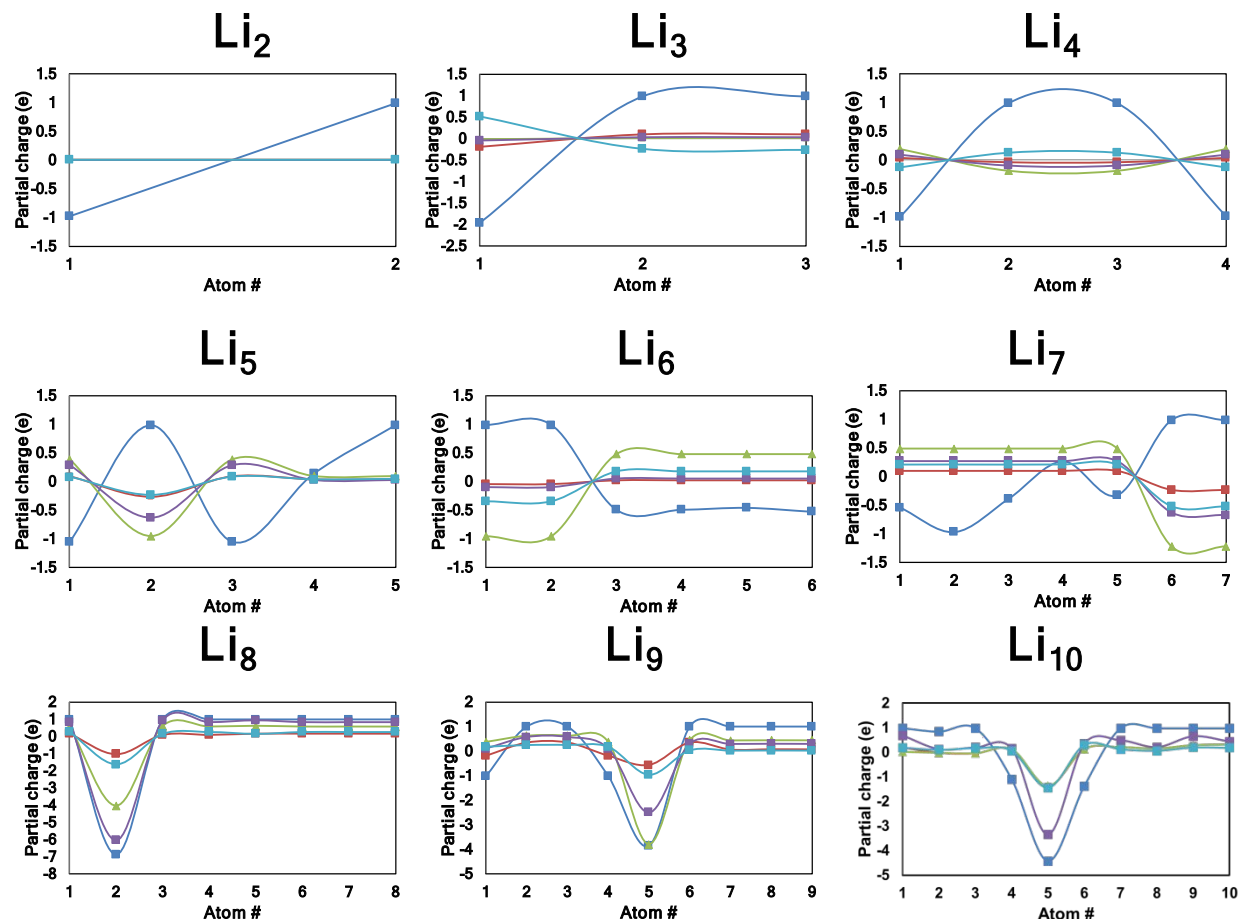


**Figure 2**: Partial Charges of $Li_x$ (for atoms labeled as x, $2 \leq x \leq 20$) clusters with Bader(blue), Mulliken (red), NBO (green), HLY (Purple) , and APT(Turquoise)

***Optimization of charged clusters.*** All the clusters were run in a neutral state. However in a battery electrode operation the charge state of the lithium anode is expected to be negative due to applied potential of the electrode. To investigate these effects, we ran the same clusters with an extra electron (Figure 3, Figure S6, Figure S7). The structures and the partial charges are similar to the neutral case.
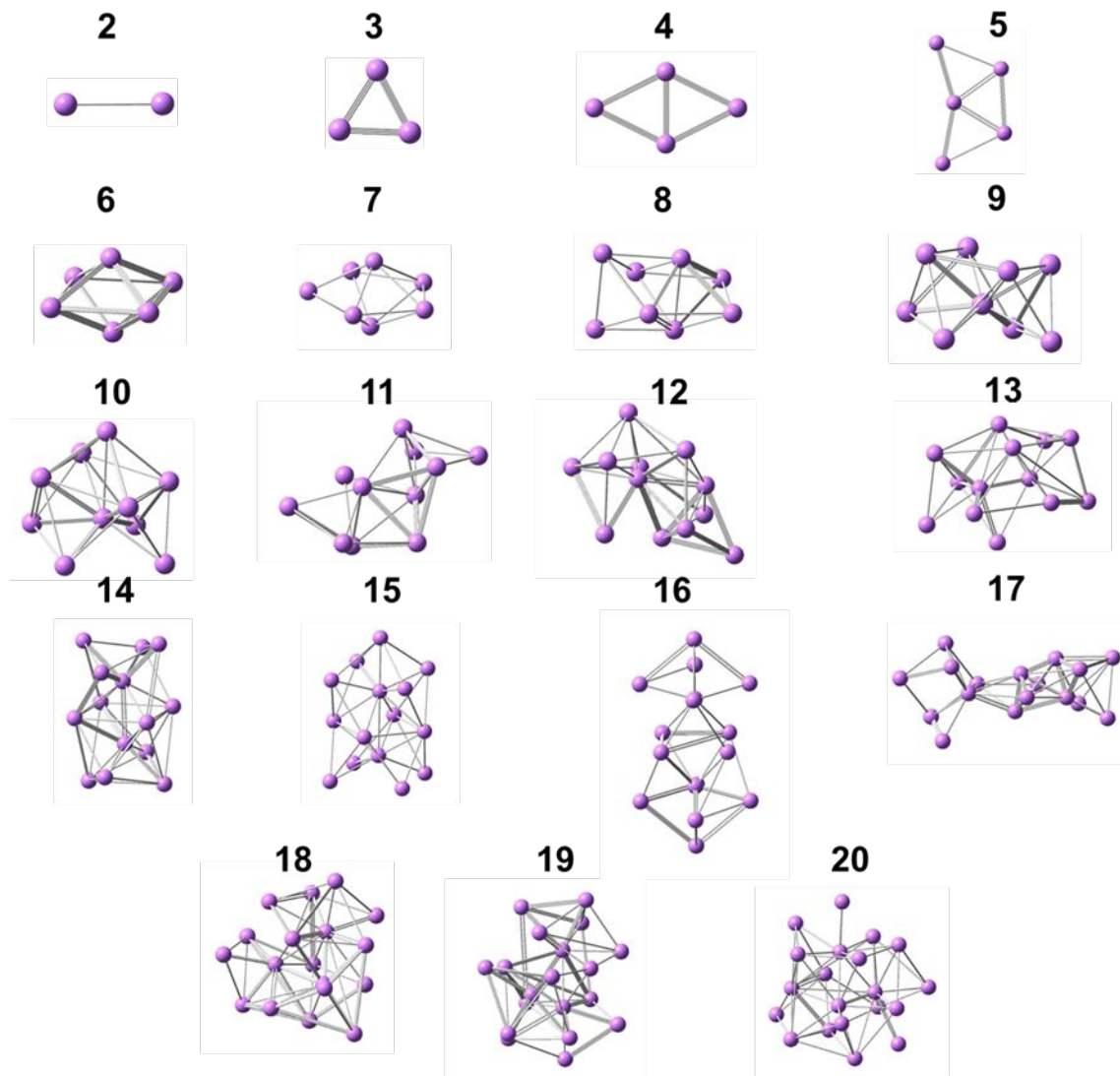
**Figure 3**: Optimized Li nanocluster structures with 1 extra electron

**Reduction of electrolyte species at the surface of the "nanoelectrodes**". These clusters may represent a "nano-electrode," which can be used to calculate the reduction potential. These simulations account for the effect of a lithium metal anode oxidizing and passing the electron to another molecule if it is favorable. The reduction of DME, LiFSI and LiTFSI were investigated with this method. DME was chosen to represent the solvent, because along with LiFSI and LiTFSI is a commonly used electrolyte in lithium sulfur battery systems in particular. LiFSI and LiTFSI were selected as lithium salts for direct comparison to previous work published by the group. The structures and color legend of the atoms are shown in Figure S12. The simulations were carried out by placing the molecule of interest near lithium clusters of size $Li_x$ (x=1,5,10,15,20) and optimized. The energies from these simulations were used for the calculation of the complex formation energy and the reduction potentials. The complex formation energy refers to the difference in free energy from the Li cluster and DME/LiTFSI/LIFSI at infinite separation to close

contact without adding or removing any electrons. For each simulation, the location of reduction was determined by using the spin density or the highest occupied molecular orbital (Figure S9). The goal of these models is to provide a simplified model to probe reductions over lithium metal.
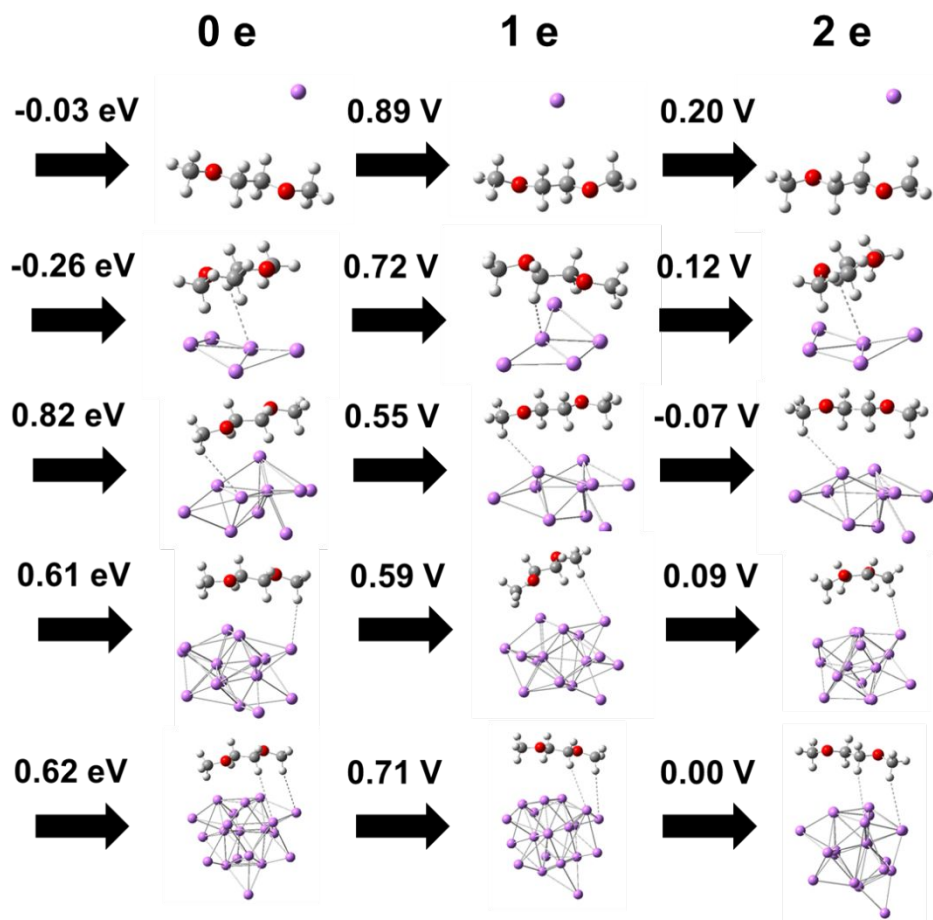


**Figure 4**: Complex formation energy (leftmost) and first and 2nd reduction potentials for Li nanoclusters with DME

One of the disadvantages of this method, is that we can detect the reduction of the lithium cluster if that is more favorable than another species. This occurs because bringing the lithium cluster to a neutral state is more energetically favorable than further reduction of the species in question. This means that which species is reduced cannot be taken for granted and must be investigated to provide meaning to the reduction potentials. Based on Table S1, DME has unfavorable reduction energetics, which the lithium cluster version of the reduction does not show. However, based on the examination of the spin densities, the additional electron in the system was localized in the Li cluster so the reduction potentials for the DME shown in the 1st reduction potentials are actually the reduction potential of a Li cluster near a DME molecule. The LiFSI and LiTFSI seem to have a lack of consistency between the different sized clusters showing a wide range of reduction

potentials. One of the reasons behind this is that even without adding electrons the neutral clusters can reduce the lithium salts. This is akin to other computational work where lithium metal slabs are placed into a system and then reduce different electrolyte species. This type of reduction is essentially the pristine lithium metal reducing the electrolyte before any passivation occurs with the formation of the SEI.  It is also in agreement with the spontaneous oxidation and dissolution of Li metal into electrolyte phases observed experimentally even in absence of any applied field.[43]

In the case of bringing DME near neutral lithium clusters, no reactions occur. As the size of the lithium cluster increases, the favorability of close contact decreases (Figure 5). This result is interpreted as the DME approaching the Li electrode in this ideal situation. One possible

DME within a close distance may be unfavorable, unless there is an electron-rich environment. [21]
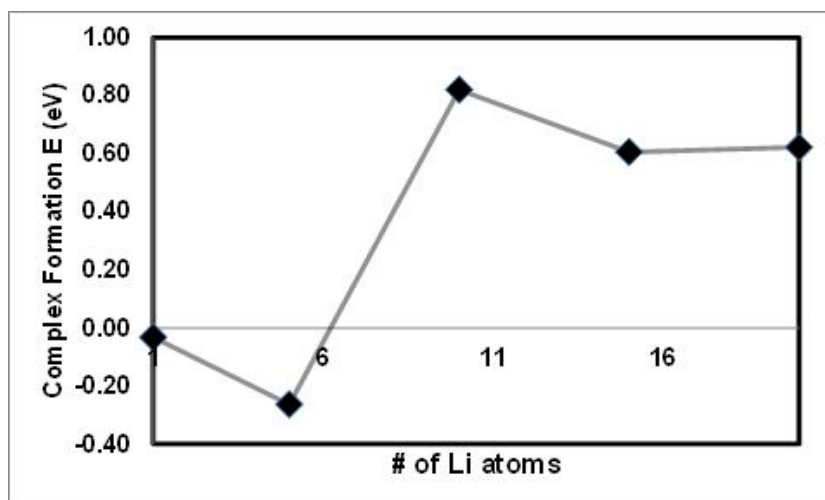


**Figure 5**: DME-Li Complex Formation Change in Free Energy
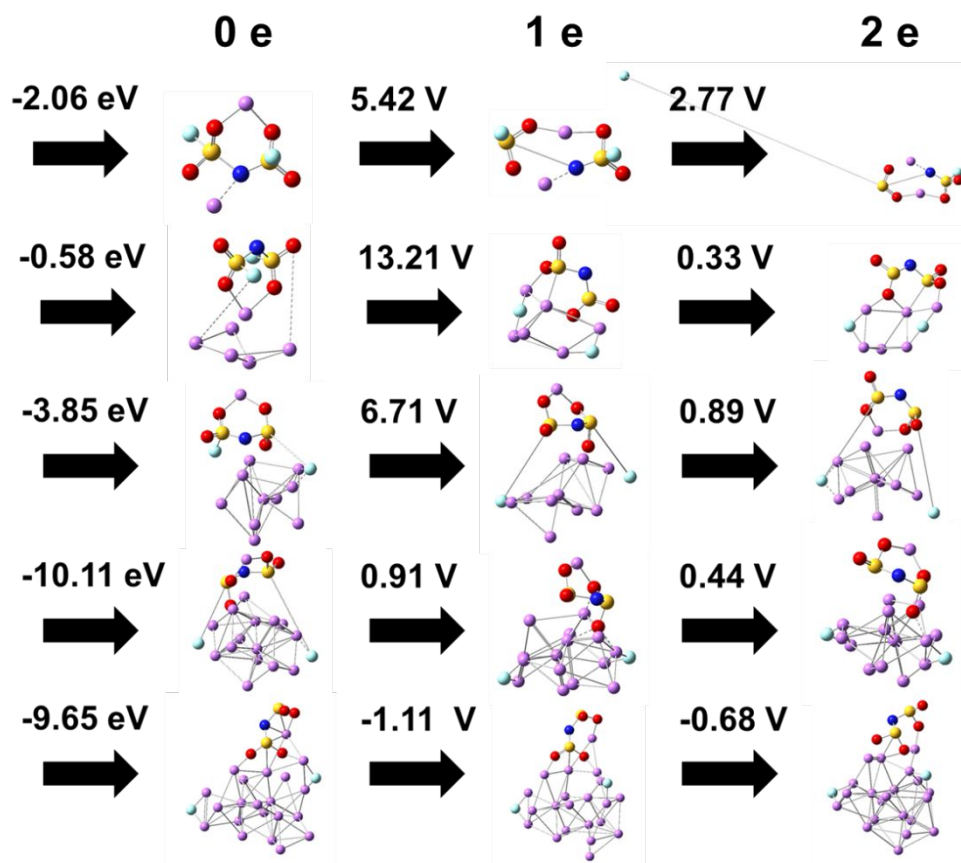
**Figure 6**: Complex formation energy and Reduction potentials for Li nanoclusters with LiFSI

The LiFSI and LiTFSI seem to have a lack of consistency between the different sized clusters showing a wide range of reduction potentials (Figures 6 and 7). One of the reasons behind this is that even without adding electrons the neutral clusters can reduce the lithium salts. This is akin to other computational work where lithium metal slabs are placed into a system and then reduce different electrolyte species. This type of reduction is essentially the pristine lithium metal reducing the electrolyte before any passivation occurs with the formation of the SEI. It is also in agreement with the spontaneous oxidation and dissolution of Li metal into electrolyte phases observed experimentally even in absence of any applied field.[43]  LiFSI-Li complex formation energies are highly negative ranging from -2 ~-10 eV (Figure 6). Unlike the DME, the LiFSI undergoes a charge transfer reaction with the lithium cluster in every single case. With the $Li_1$ cluster, the Li atom is oxidized and the electron is given to the LiFSI, but no bonds were broken. In the $Li_5$ case, the $Li^+$ from the LiFSI is oriented close to the cluster and reduced. The $Li_{10}$, $Li_{15}$, $Li_{20}$ simulations show the LiFSI molecule bond breaking and forming smaller fragments. The complex formation energy of -3.85 eV is associated with one F breaking off and ~-10 eV for 2 F atoms reduction. This can be compared to reduction simulations without the Li nanoclusters such as those shown in Table S5. In orientation 7 (Table S5), the FSI anion was reduced with a potential ~3 V which is within 1 V of the observed reduction of 3.85 V with the Li cluster. The energies

should be similar but likely not the same since there are other effects like the stabilization of the fragments by the lithium cluster that need to be considered. With the lithium clusters, the energy it takes to remove an F atom from the LiFSI is ~4 eV and when two are removed the energy is ~10 eV or ~5 eV/F atom. These numbers are relatively comparable. The seemingly random energies for LiFSI-Li complex formation are not as chaotic as they seem once examining the reactions that occur.
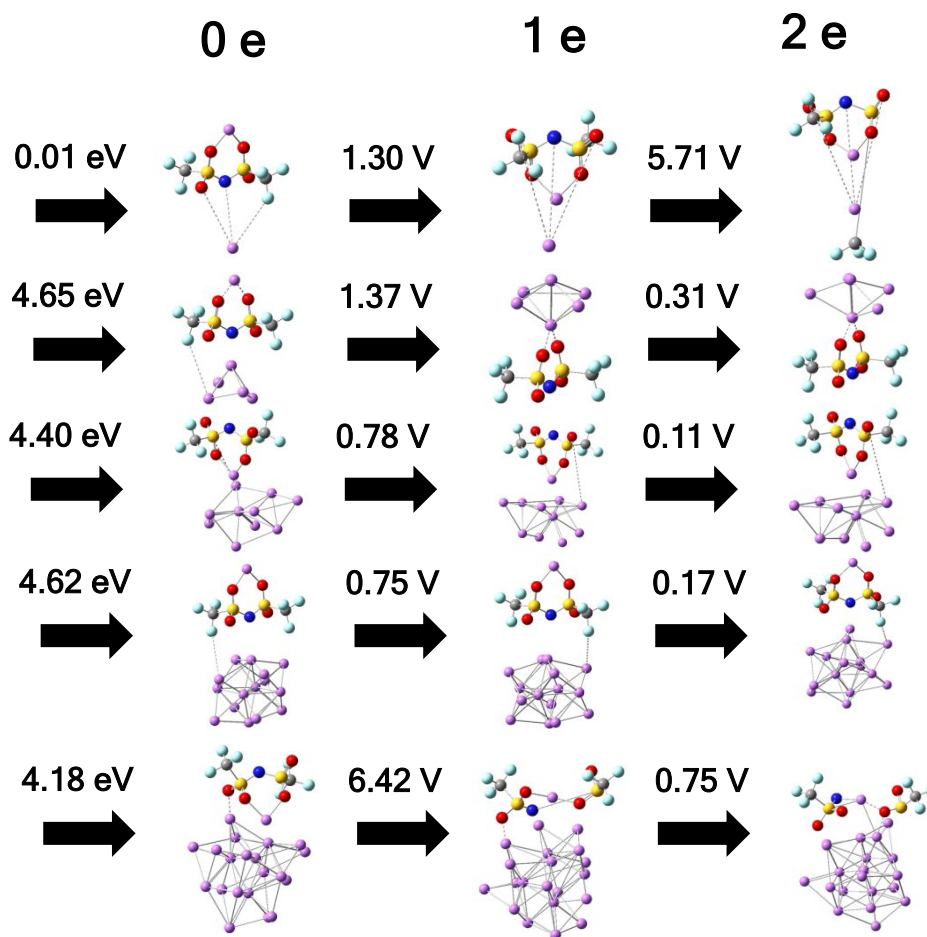


**Figure 7**: Complex formation energy and Reduction potentials for Li nanoclusters with LiTFSI

For LiTFSI, no reactions occur just like with the DME (Figure 7). Another interesting property of the LiTFSI system is that in every case but the $Li_1$ cluster, the formation of the LiTFSI-Li complex is not thermodynamically favorable. LiTFSI is known to be less reactive than LiFSI which this result confirms. Since both DME and LiTFSI have mostly unfavorable formation energies with Li clusters, perhaps LiFSI does as well but the energies are favorable due to the electron transfer from the cluster. Essentially, the stability of the LiFSI reduction products drive the complex formation

of the LiFSI-Li and the reduction. Since the transfer occurs spontaneously, there is no simple way to calculate the LiFSI without the electron transfer.

The 1st and 2nd reduction energies were simulated for the same clusters. With DME (Figure 4), all of the 1st and 2nd reduction reactions reduce the Li cluster except the 2nd reduction of the DME-Li1 system. For the 1st reduction potential, the values are in the range of 0.5-0.9 V which is associated with the reduction of the Li cluster. These values are quite similar to those simulated without the lithium clusters. The 2nd reduction potentials are lower in magnitude for all the cases including the DME reduced case. The LiFSI reductions (Figure 6) once again show large differences between simulations of different cluster sizes. These numbers are closely related to the reactions that are actually occurring. With the $Li_1$, the LiFSI is reduced breaking a S-N bond which is associated with a potential of ~5.5 V. The $Li_5$ simulation has a potential of 13.21 V which is associated with two F atoms being broken off the LiFSI. In the $Li_{10}$ case, another fluorine atom is removed and in the $Li_{15}$, the lithium cluster is reduced which provides a much lower reduction potential ~ 1 V. The reduction of the lithium cluster can be thought of as the cluster being brought to a charge neutral state after the reduction of the LiFSI. Since the size of the clusters is small and dissolution of a $Li^+$ is not possible, it might be more energetically favorable to reduce a lithium than the salt further. The 2nd reduction potentials all occur to the lithium cluster except the LiFSI-$Li_1$ simulation where a fluorine atom is broken from the LiFSI. In previous studies of the decomposition of LiFSI over Li metal, the fluorine atom was reported to be broken off of the LiFSI molecule quite favorably.[30] In that particular study, a solid state model of lithium was used which provides a comparison between reductions with the nanocluster versus a more accurate but more computationally expensive system.

The reactions have a similar order of magnitude (4-6 V for fluorine atom, 0.5-1 for Li reduction) but the numbers do show variability. These differences can be due to configuration of different components and stabilization of reduction products with the lithium cluster. For instance, in the case of LiFSI-$Li_5$ 1st reduction, two fluorine atoms are broken off of the LiFSI, but the potential is more favorable than in the complex formation cases (Figure 6) . This could be due to $Li^+$ of the salt being incorporated into the lithium cluster. As demonstrated throughout this work, configurational changes can have a strong impact on results. The other possibility is demonstrated by the LiFSI-$Li_1$ simulation. The LiFSI molecule is reduced breaking off a fluorine atom, which separates itself from the salt by a large distance. The potential associated with this is ~ 3 V which is lower than the other reductions with the same species. In those cases, the fluorine atom moves to a different location on the lithium cluster which can be thought of as forming LiF. This stabilizes the fluorine atom therefore the reduction potential increases.

The same analysis is repeated for the LiTFSI (Figure 7). In the 1st reduction potentials, three different reduction locations occurred. One is the $Li^+$ of the LiTFSI with a potential of ~1 V, second is the lithium cluster with a lower V than the previous and the final location is the TFSI anion itself with the highest potential of ~ 7 V. The reduction potential of the TFSI anion is higher than that found with the implicit solvent but the location is different as well. The S-N bond was broken

instead of S-C. In the 2nd reduction potential simulations, the electron is assigned to the lithium cluster in most cases except the LiTFSI-Li$_1$ case. In this simulation, a CF$_3$ group is fragmented off the molecule and moves to a position near the lithium "cluster". The bond breaking of a CF$_3$ group off LiTFSI was characterized in previous work showing that this is the most likely bond to be broken in the molecule[30]. This has also been observed in experiments and simulations with the presence of SEI. Though the SEI passivates the reduction, when the LiTFSI is transferred electrons , the cleavage of the S-C bond is observed.[23] The associated reduction potential is noticeably higher than in the implicit cases which are likely due to the stabilization effects of the lithium cluster.

In summary, these models predict similar reduction behavior of these molecules as previously published computational studies while taking a fraction of the computational cost. The models also incorporate important energies caused by the presence of a lithium metal electrode that is normally difficult to incorporate into computational models while still being able to obtain results in a facile manner. Other computational models provide different insight into other effects such as diffusion barriers and binding energies.[44] Together with other experiments and models, the nanoclusters allow for accurate and inexpensive insight into reactions that are critical to the formation of the SEI and properties of a lithium metal electrode.

**Nucleation and Growth of Lithium Dendrites**

As with the SEI, lithium dendrites have been the focus of much study experimentally and computationally. These studies have ranged from mitigation methods to exploring the fundamental nature behind what causes dendrite growth.  Probing the underlying mechanisms behind dendrite nucleation and growth is absolutely critical to understanding the problem so that a strategy to finding as solution can be developed. Most work into the fundamental nature of dendrites has been spent at the meso-scale level of simulation. These types of models provide insight into the continuum level behavior of lithium deposition and are able to demonstrate the growth of dendrites from one electrode and observe branching and other effects. They also allow for exploration of what variables will affect the behavior of dendrites. However, there has been very little information at the formation of dendrites at an *ab-initio* scale. Though the scale at this level is restricted every chemical process is governed by quantum level in one way or another. The clusters presented in the previous section also can be used to explore dendrites at an absolute fundamental scale.

Though the lithium clusters simulated are the most stable from an energetic viewpoint, when considering the lithium reduction and thus nucleation of a dendrite, the relative timescales of kinetics versus thermodynamics come into play. Given enough time to reach equilibrium, the lowest energy structures of the lithium nanoclusters will be present but if the deposition of Li$^+$ ions occurs quickly enough then the progress towards the favored equilibrium structures will be changed. If the timescale of the kinetics is slower, then the thermodynamics should predict the structures. Though much is understood about the formation and growth of Li dendrites, there is little information about it from a first principles perspective. Li dendrites have to nucleate from

atoms at some point so understanding this is vital to building up models and the theory to stop the growth of Li dendrites.

Assuming that a $Li^+$ ion can approach the Li cluster from any direction, there are unique addition spots where the $Li^+$ could be reduced. The $\Delta G_{reduction}$ was calculated for the clusters with a $Li^+$ at each of these locations. The lower the $\Delta G_{reduction}$ the more favorable the reduction, which is the thermodynamically favored addition to the Li cluster. The results and corresponding snapshots are in the Figure S2.

For the tested cases, the $\Delta G_{reduction}$ was very similar within reasonability that the different reduction sites are essentially thermodynamically equivalent. Based on these calculations, the expected nucleation and growth of the clusters is nonspecific. Some of the structures in Figure S2 are the same as the most energetically favored structures in Figure 1, but not all of them are the same. The theory is that the reduction would occur at the site of the lowest $\Delta G_{reduction}$ and then the cluster would rearrange or another process will take place to minimize its free energy. Given that the energetics of $Li^+$ addition and reduction with the cluster are favorable at all sites, we determined that there won't be any directionality to the growth based on this method. In this model the lithium will reorganize and form "spherical" structures. In an actual battery, there will be a lithium metal electrode instead of free-floating lithium clusters but even in those cases, the thermodynamic favorable state should approach bulk Li metal, which does not provide for any directionality.

***Evaluation of electrostatic potentials.*** The $Li^+$ ions are solvated by the electrolyte and under the influence of several forces such as chemical potential driven mass transfer, electric fields from the electrodes and other electrostatic interactions. Assuming that a $Li^+$ ion is able to approach the nanocluster from the bulk solvent, how will the $Li^+$ approach the Li cluster? From the $\Delta G_{reduction}$ calculations, once the $Li^+$ is close enough to the cluster then the reduction and charge transfer will occur. The important forces guiding the $Li^+$ ion in the range between bulk solvent and reduction distance will be electrostatic interactions which will come from two places: the electrostatic potential (ESP) and electric field from the electrode. Attractive interaction will force the $Li^+$ ion in a particular direction and once the ion is close enough reduction will occur.
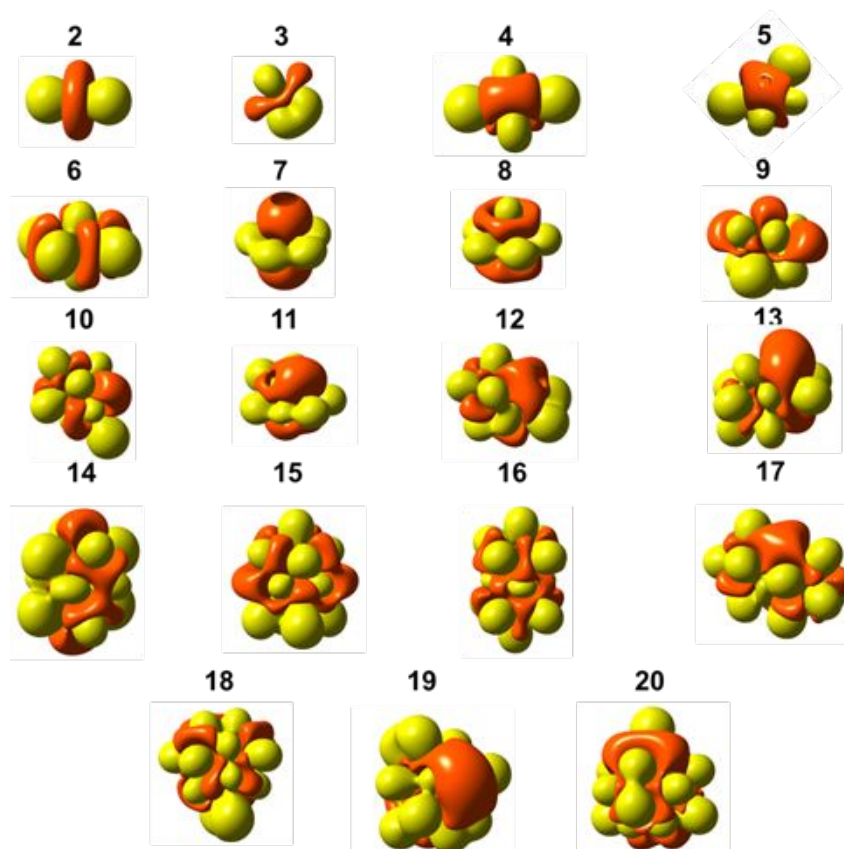
**Figure 8** : Electrostatic potentials for $Li_x$ clusters. Orange is negative, Yellow is positive. Isosurface value of .008 au

We first explored this concept by visualizing and quantifying the ESP of the Li nanoclusters (Figure 8). The negative parts of the ESP will be attractive to the $Li^+$ ion while the positive parts will be repulsive. Based on this model, the $Li^+$ ions will be reduced at where they are guided to by the ESP. The shape of the ESPs of the clusters follows a general pattern that the ESP is always repulsive over Li atoms and attractive over the rest of the cluster. This can be reworded as the ESP is attractive to the $Li^+$ ions at interstitial locations. This trend is observed in all of the 10 clusters analyzed. The electrostatic potential for the negative clusters were also examined (SI) to represent a potential being applied. The magnitude of the ESP is more negative/attractive but the shape is the same. This means that in a negative cluster the whole cluster is attractive but some parts are more attractive than others just like in the neutral case.

***Effect of an electric field on the electrostatic potential.*** The ESP will not be the only force acting on the $Li^+$ because of the presence of an electric field at the interface of the electrode. These effects can be estimated by including an additional electric field in the simulations. Figure S10 shows the structures and ESP for nanoclusters with an electric field added to the simulation. The presence of the electric field is clear on the ESP. Throughout the entire simulation area, the ESP has more

negative values and the ESP is shifted in the spatial direction that the field is applied in. The general shape of the ESP is the same except some sides of the clusters are promoted over others.
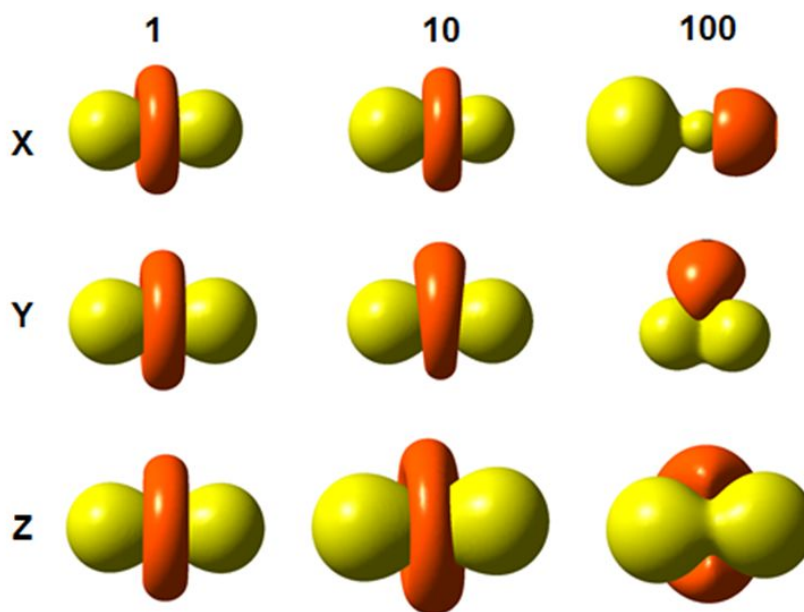


**Figure 9**: $Li_2$ cluster electrostatic potential with external electric field applied to x,y and z direction with strengths of 0. 0001, 0. 001 and 0.01 au. Orange is attractive and yellow is repulsive. Isosurface values of 0.008,0.008,0.02 respectively.

Using this information about the shape and magnitude of the Li cluster's ESP with and without and electric field, we executed new $Li^+$ ion addition and reduction calculations. Instead of placing the Li ions in unique locations anywhere on the cluster, Li ions were only placed at unique sites that had a negative ESP. Figure S3 shows the results of the Li cluster evolution via this methodology. For the most part, the $Li^+$ ion additions gave the energetically favored structures (Figure 1) but some of the structures differed. These alternative Li cluster configurations were compared in energy to the most stable and the differences were negligible (Table S9). This demonstrates that even though some Li cluster configurations may not be the lowest energy, they are not largely unfavorable from an energetic perspective.

*Model of growth evolution.* Unfortunately, a computational chemistry program can only handle so many electrons before the simulations become unsolvable. This leaves something to be desired since to even observe a hint of dendrite nucleation, larger cluster sizes are needed. This requires another method based on ab-initio information that can be used to create larger clusters. The behavior of the ESP with and without an external field presents an interesting generalization. The ESP behavior follows one rule and the structures created by this rule are very similar in energy to the thermodynamically preferred configurations. Based on this, we built an evolution model that is computationally inexpensive and allows for the growth of large Li clusters (# of Li ~5000 or less). This model does not account for many effects such as the role of SEI. The goal of this model

is to obtain a base understanding of factors that may effect dendrite growth so a highly simplified model is required.

An internal program was created in Matlab to build or evolve Li clusters based on the assumption that a Li will always add to an interstitial site and that each interstitial site is just as likely to have an Li added to it. The other assumptions are that the generalization of the ESP holds and that the energetics of these configurations are still similar in energy to the minimum energy configuration. The simulation works by starting with a $Li_3$ cluster arranged in a triangle. Then the program randomly selects a valid triangle hollow site and adds a Li to the make a trigonal pyramid structure. This process is repeated until the number of Li atoms specified is reached. In order to study the statistics of the configurations, we ran the simulation 100 and 1000 times to observe the likelihood of configurations.

Since we are interested in the nucleation of dendrites, we characterized the configurations of lithium based on acentricity or the deviation from a spherical configuration. Our acentricity factor was defined by determining the variance in the radius of the outer Li atoms normalized by the number of total Li atoms. The more acentric the cluster is, the more interesting as a potential dendrite nucleation mechanism. The most acentric case for a $Li_{500}$ is shown in Figure 10. The cluster shown is quite acentric and rectangular in nature. As a contrast, the most spherical case is shown in Figure 11.
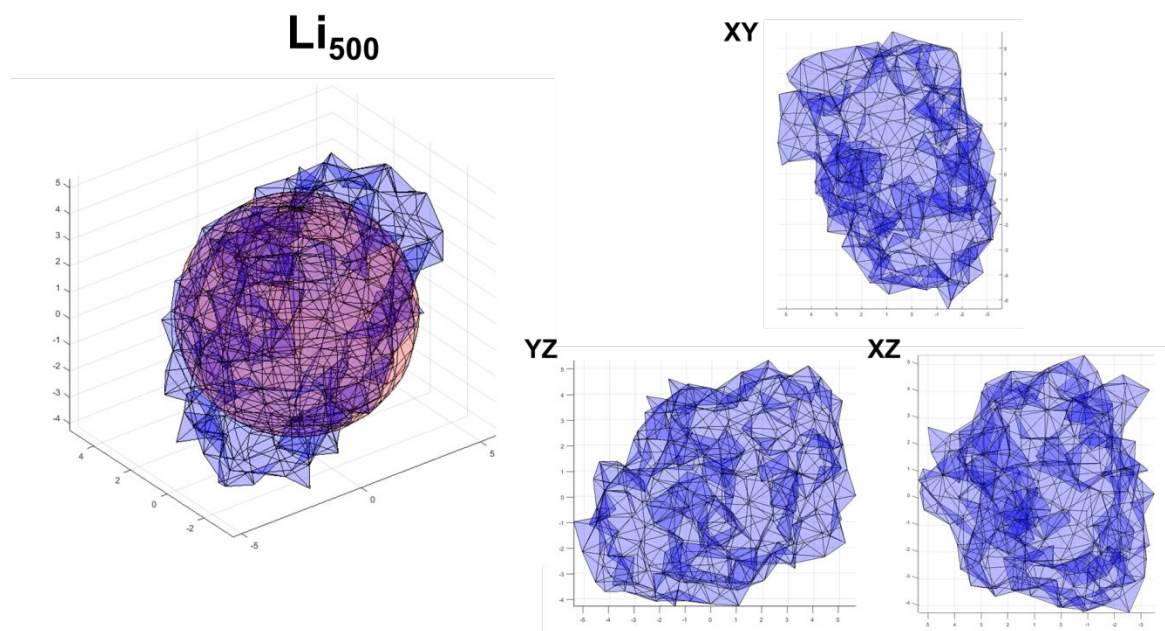


**Figure 10**: Most acentric $Li_{500}$ cluster with 1000 trials. Blue is surface of cluster, orange is a unit sphere to provide perspective
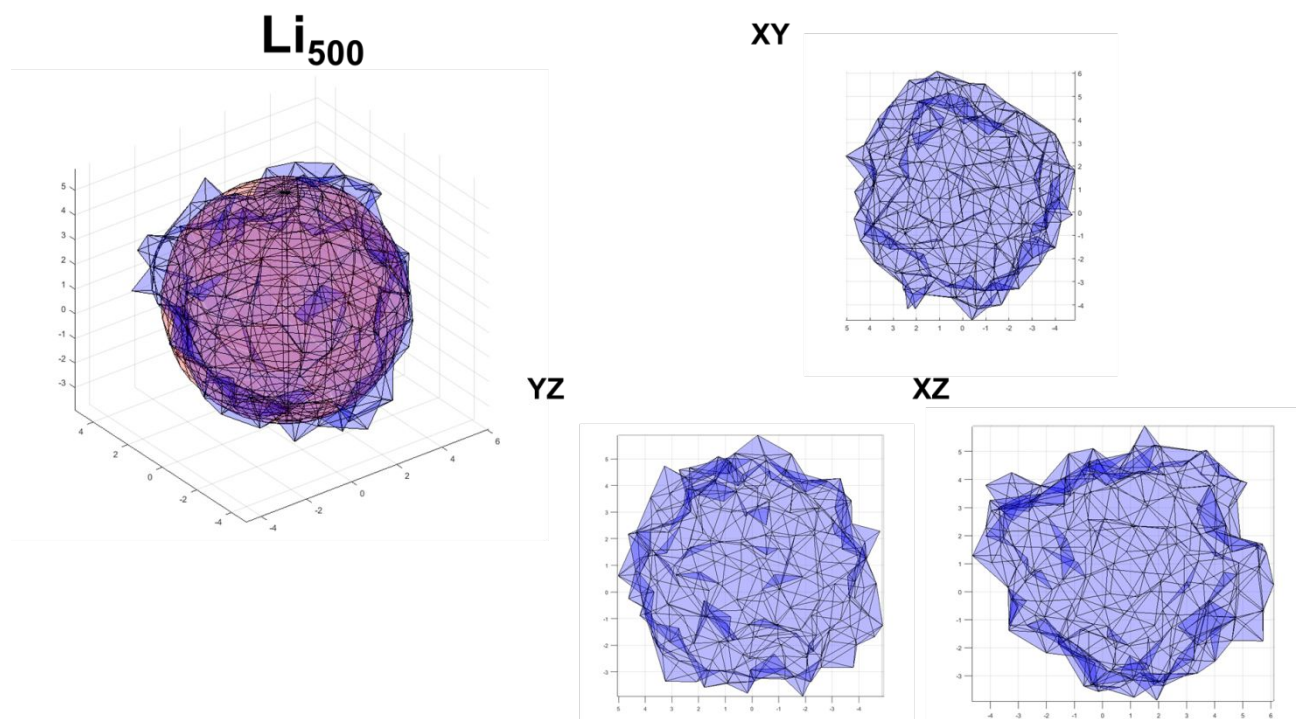
**Figure 11**: Least acentric $Li_{500}$ cluster with 1000 trials

The acentricity metric does not always provide the best view of dendritic like growth. We observed in many cases that the most acentric structures were sometimes spheroidal in nature but the variance in radius was high due to a "rough" surface. In addition to the acentricity of the structures, the aspect ratio was examined to determine a rectangular acentricity. The aspect ratio was defined as taking the shortest dimension divided by the longest dimension of the cluster. This metric was far more successful at finding structures that were better descriptors of dendrites. For the $Li_{500}$ with 1000 trials, the most rectangular was also the least spheroidal shape. For the $Li_{250}$ cluster, this is not the case and the results are shown below.
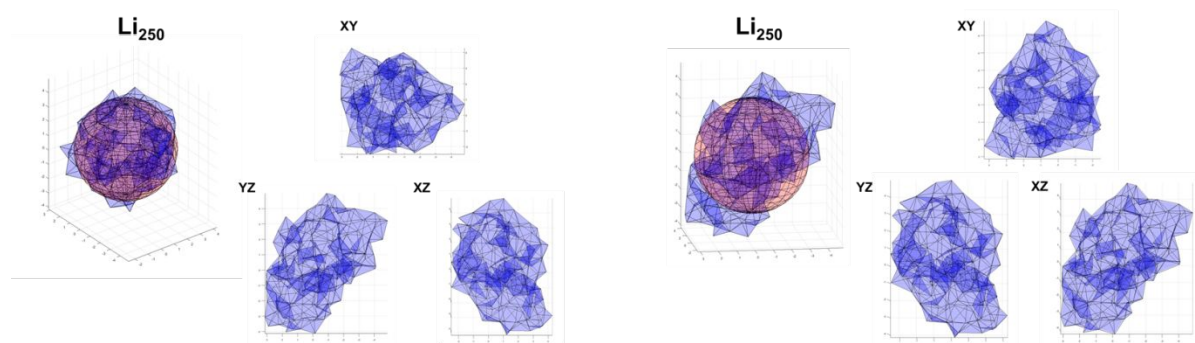


**Figure 12**: $Li_{250}$ with 1000 trials. The left structure shows the most acentric case. The right structure shows the most rectangular case.

In Figure 12, the most rectangular case has an appearance that is highly suggestive of a small lithium dendrite. From visual observation, it is clear that dendritic like lithium clusters can be formed from the simplified assumptions used to create this model. Even in the absence of electric fields, solvents, and other important physical and chemical factors, dendrites are able to be formed just from the geometry of nucleation and an interstitial electrostatic potential. The question becomes, how often do these highly acentric and rectangular lithium clusters arise? Figure 13 contains the histograms for acentricity and rectangularity for the $Li_{250}$ case. Both histograms resemble normal distributions but the rectangular acentricity has a longer right tail. These results demonstrate that the most acentric and rectangularly acentric cases are not the most common structures. However, it only takes a relatively few number of dendrites to ruin a battery's performance. Also on the atomic scale, there will be more than 1000 "trials" for a dendrite to form. Once a dendrite is formed, it will be more accessible for further lithium reduction and become a larger problem.
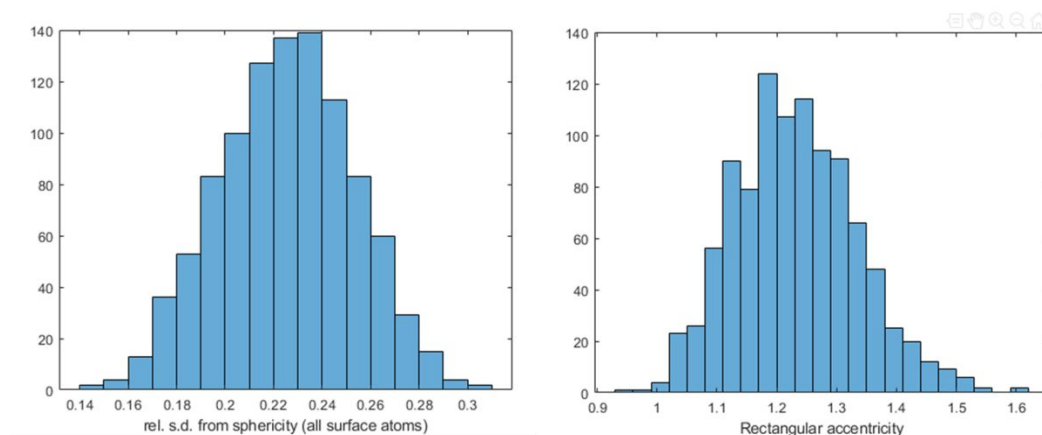


**Figure 13**: $Li_{250}$ with 1000 trials histograms The left histogram represents the spherical acentricity and the right histogram represents the rectangular acentricity.

These models demonstrate that with very few assumptions, highly abnormal geometric shapes of lithium can be formed based on available reduction sites and randomness. One detail that this model overlooks is that in any normal battery, the nucleated structure in general does not start as a triangle in space or grows in a spherical geometry. To address this, the code from the previous figures was adapted to start with a square surface and restrict the acceptable domain for addition to be bounded by the starting square and only allowing positive Z growth. For these, simulations, less trials were run due to more computational complexity but the trials with the highest Z value were selected as the most dendritic cases.
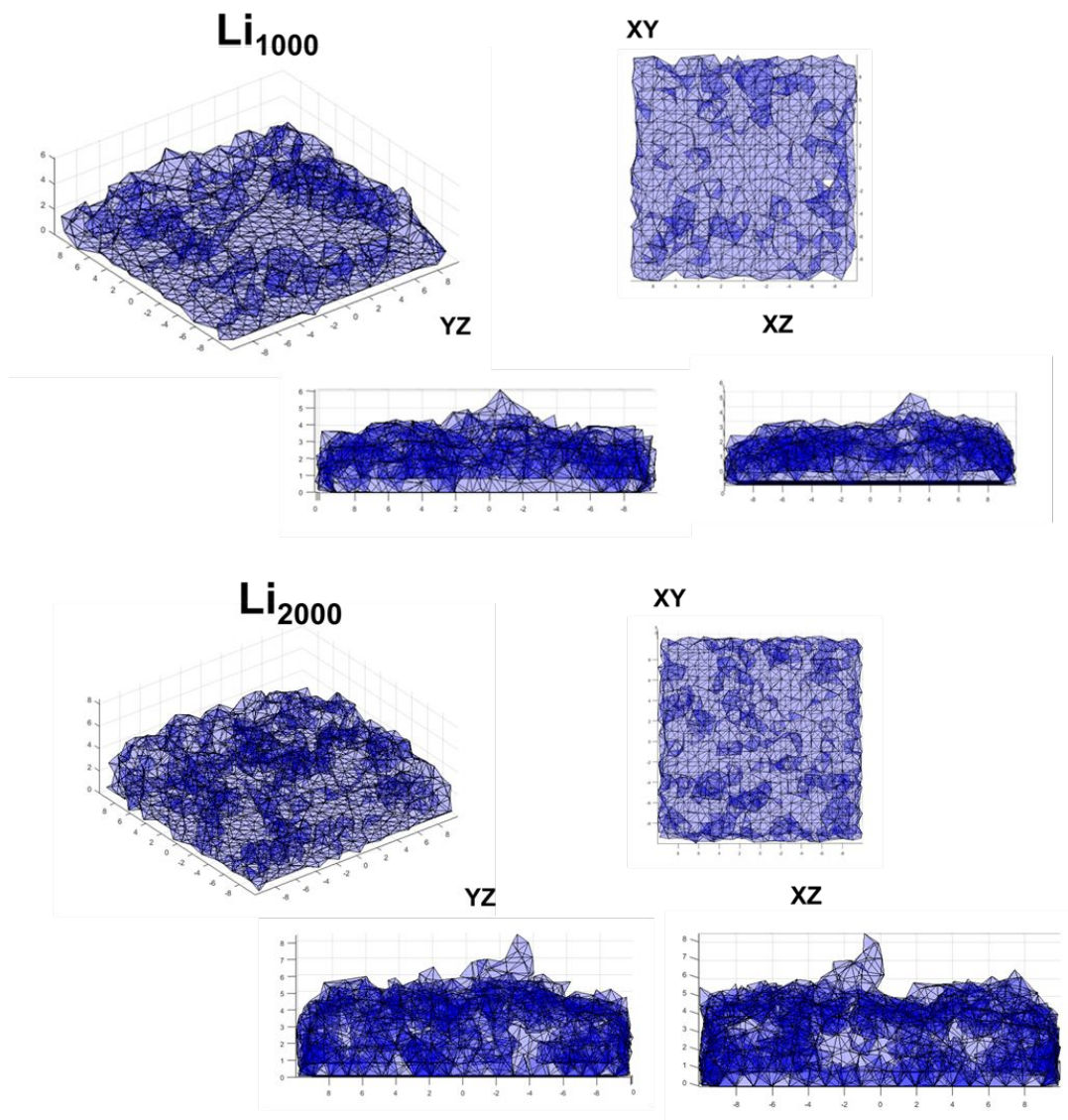
**Figure 14**: The top structure shows the $Li_{1000}$ electrode largest dendritic growth case. The bottom structure shows the $Li_{2000}$ electrode largest dendritic growth case.

In both cases most of the lithium is added in a uniform manner but there are definite spikes or dendrite like structures that have started to form. The nucleation of dendrites was not limited to the spherical growth case. These simulations demonstrate that with very few rules based on the ESP from first principles simulations, dendritic structures have been observed in the electrode like starting structure as well. This gives important insight into the fundamentals of lithium dendrite nucleation and growth and mitigation strategies to counteract dendrites. Based on this model, solutions to changing how dendrites grow should focus on manipulating the electrostatic potential whether by insulating or ensuring homogeneity. The results from this model also fit into the previously mentioned meso-scale computational studies. These studies have shown that where there is a hot spot of current, or available surface area from a crack in the SEI, Li dendrites will

grow there. In many ways, the attractive ESP represents a rough approximation to the available surface area of the cluster. This additional insight into which factors matter at an ab-initio level provide a framework to screen and create an encompassing strategy to mitigating lithium dendrites.

## Conclusions

First principles models can be used to assist in processing and screening the nearly limitless amount of research directions for next generation batteries. These models provide fundamental details of an electrochemical system that can be difficult or impossible to determine experimentally. Though many computational models are highly complicated, and time consuming, simpler model systems are needed in order to effectively make quick progress.

Here we report a methodology for a simple model that can be used to screen reduction potentials of different compounds with an improved accuracy cluster-continuum solvation model. The inclusion of explicit solvent molecules can significantly change the outcome of the reduction calculation which is why the solvent molecules must be included. This model provides a basis for exploration and screening of many different electrolyte compounds and chemistries. To include the effects of an electrode thus increasing the physicality of the model, we built lithium nanoclusters to represent larger electrodes. These clusters were characterized by different partial charge analysis techniques to determine the most reasonable and the clusters were used to explore the reduction of LiTFSI, LiFSI and DME. The reduction results show good comparison with previous computational work done on the topic and provided new insights regarding the role of the electrode. The lithium nanoclusters also allowed for a first principles perspective of the growth and nucleation of lithium dendrites. Based on the reduction thermodynamics, there is no directionality to the growth of a lithium cluster which indicates that other forces may be more important. We looked toward the ESP to provide a roadmap for the growth of a lithium dendrite. From the first principles simulation, a non ab-initio model was created in MATLAB to build much larger lithium clusters than what first principles programs are capable of. With very few assumptions, the MATLAB code was able to nucleate and grow structures that were abnormal and dendritic in nature thus giving some insight into the fundamentals of lithium dendrite formation.

For future work, the current models will be used to investigate more species of interest for battery chemistry such as carbonate-based and localized-high concentration electrolytes and additional lithium salts using the models and procedures reported here. We also plan to extend the models reported here in the future to include other important effects that will extend the models. The inclusion of SEI molecules on the lithium nanoclusters will allow for the study of the passivation and interactions that the SEI will introduce. The effects of the SEI can also be introduced into the dendrite model as well based on how the inclusion of different SEI components changes the ESP that the model is based on.

## Supporting Information

The following material is available free of charge: Reduction of electrolyte components in absence of a Li cluster (Tables S1 to S8; Fig. S1); $Li^+$ insertion and reduction pathways for Li clusters up to 10 atoms based on thermodynamic calculations (Fig. S2); Evolution of Li clusters based on electrostatic potential (Fig. S3); Electrostatic potential isosurfaces for neutral clusters (Fig. S4); Total Electron Densities for neutral Li Clusters (Fig. S5); Electrostatic Potentials for Li clusters with 1 additional electron (Fig. S6); Total Electron Densities for Li clusters with 1 additional electron (Fig. S7); Geometry, electrostatic potential and total electron density respectively for subset of Li clusters with 1 electron removed (Fig. S8); Structures, spin densities, reduction or complex formation energies and HOMO isosurface for all Li reductions (Fig. S9); Electrostatic potential of Li clusters up to 10 atoms with external field applied (Fig. S10); Most Acentric Case for Li1000 electrode Model (Fig. S11); Molecular structures (Fig. S12)

*References*

1.      Lin, D.;  Liu, Y.; Cui, Y., Reviving the lithium metal anode for high-energy batteries. *Nature nanotechnology* **2017,** *12* (3), 194.
2.      Amanchukwu, C. V.;  Gauthier, M.;  Batcho, T. P.;  Symister, C.;  Shao-Horn, Y.;  D'Arcy, J. M.; Hammond, P. T., Evaluation and stability of PEDOT polymer electrodes for Li–O2 batteries. *The journal of physical chemistry letters* **2016,** *7* (19), 3770-3775.
3.      Tang, X.;  Xu, Z.;  Sun, Z.;  Zhou, J.;  Wu, X.;  Lin, H.;  Rong, J.;  Zhuo, S.; Li, F., Factors of Kinetics Process in Lithium-Sulfur Reaction. *Energy Technology*.
4.      Wang, A.;  Kadam, S.;  Li, H.;  Shi, S.; Qi, Y., Review on modeling of the anode solid electrolyte interphase (SEI) for lithium-ion batteries. *npj Computational Materials* **2018,** *4* (1), 15.
5.      Xu, L.;  Tang, S.;  Cheng, Y.;  Wang, K.;  Liang, J.;  Liu, C.;  Cao, Y.-C.;  Wei, F.; Mai, L., Interfaces in solid-state lithium batteries. *Joule* **2018,** *2* (10), 1991-2015.
6.      Liu, Y.;  Lin, D.;  Yuen, P. Y.;  Liu, K.;  Xie, J.;  Dauskardt, R. H.; Cui, Y., An artificial solid electrolyte interphase with high Li-ion conductivity, mechanical strength, and flexibility for stable lithium metal anodes. *Advanced Materials* **2017,** *29* (10), 1605531.
7.      Aurbach, D.;  Zinigrad, E.;  Cohen, Y.; Teller, H., A short review of failure mechanisms of lithium metal and lithiated graphite anodes in liquid electrolyte solutions. *Solid state ionics* **2002,** *148* (3-4), 405-416.
8.      Agubra, V. A.; Fergus, J. W., The formation and stability of the solid electrolyte interface on the graphite anode. *Journal of Power Sources* **2014,** *268*, 153-162.

9.      Xing, L.; Wang, C.; Xu, M.; Li, W.; Cai, Z., Theoretical study on reduction mechanism of 1, 3-benzodioxol-2-one for the formation of solid electrolyte interface on anode of lithium ion battery. *Journal of Power Sources* **2009,** *189* (1), 689-692.

10.     Soto, F. A.; Ma, Y.; Martinez de la Hoz, J. M.; Seminario, J. M.; Balbuena, P. B., Formation and growth mechanisms of solid-electrolyte interphase layers in rechargeable batteries. *Chemistry of Materials* **2015,** *27* (23), 7990-8000.

11.     Sacci, R. L.; Black, J. M.; Balke, N.; Dudney, N. J.; More, K. L.; Unocic, R. R., Nanoscale imaging of fundamental Li battery chemistry: solid-electrolyte interphase formation and preferential growth of lithium metal nanoclusters. *Nano letters* **2015,** *15* (3), 2011-2018.

12.     Kamyab, N.; Weidner, J. W.; White, R. E., Mixed Mode Growth Model for the Solid Electrolyte Interface (SEI). *Journal of The Electrochemical Society* **2019,** *166* (2), A334-A341.

13.     Wang, D.; Zhang, W.; Zheng, W.; Cui, X.; Rojo, T.; Zhang, Q., Towards high-safe lithium metal anodes: suppressing lithium dendrites via tuning surface energy. *Advanced Science* **2017,** *4* (1), 1600168.

14.     Liu, K.; Liu, Y.; Lin, D.; Pei, A.; Cui, Y., Materials for lithium-ion battery safety. *Science advances* **2018,** *4* (6), eaas9820.

15.     Seh, Z. W.; Kibsgaard, J.; Dickens, C. F.; Chorkendorff, I.; Nørskov, J. K.; Jaramillo, T. F., Combining theory and experiment in electrocatalysis: Insights into materials design. *Science* **2017,** *355* (6321), eaad4998.

16.     Laskin, J.; Johnson, G. E.; Warneke, J.; Prabhakaran, V., From Isolated Ions to Multilayer Functional Materials Using Ion Soft Landing. *Angewandte Chemie International Edition* **2018,** *57* (50), 16270-16284.

17.     Wei, B.; Lu, X.; Voisard, F. d. r.; Wei, H.; Chiu, H.-c.; Ji, Y.; Han, X.; Trudeau, M. L.; Zaghib, K.; Demopoulos, G. P., In Situ TEM Investigation of Electron Irradiation Induced Metastable States in Lithium-Ion Battery Cathodes: Li2FeSiO4 versus LiFePO4. *ACS Applied Energy Materials* **2018,** *1* (7), 3180-3189.

18.     Persson, M., Electric potentials at the atomic scale. *Nature materials* **2019**, 1.

19.     Li, N. W.; Shi, Y.; Yin, Y. X.; Zeng, X. X.; Li, J. Y.; Li, C. J.; Wan, L. J.; Wen, R.; Guo, Y. G., A flexible solid electrolyte interphase layer for long-life lithium metal anodes. *Angewandte Chemie International Edition* **2018,** *57* (6), 1505-1509.

20.     Nandasiri, M. I.; Camacho-Forero, L. E.; Schwarz, A. M.; Shutthanandan, V.; Thevuthasan, S.; Balbuena, P. B.; Mueller, K. T.; Murugesan, V., In situ chemical imaging of solid-electrolyte interphase layer evolution in Li–S batteries. *Chemistry of Materials* **2017,** *29* (11), 4728-4737.

21.     Camacho-Forero, L. E.; Balbuena, P. B., Elucidating electrolyte decomposition under electron-rich environments at the lithium-metal anode. *Physical Chemistry Chemical Physics* **2017,** *19* (45), 30861-30873.

22.     Guan, P.; Liu, L.; Lin, X., Simulation and experiment on solid electrolyte interphase (SEI) morphology evolution and lithium-ion diffusion. *Journal of The Electrochemical Society* **2015,** *162* (9), A1798-A1808.

23.     Kamphaus, E. P.; Angarita-Gomez, S.; Qin, X.; Shao, M.; Engelhard, M.; Mueller, K. T.; Murugesan, V.; Balbuena, P. B., Role of inorganic surface layer on solid electrolyte interphase evolution at Li-metal anodes. *ACS applied materials & interfaces* **2019,** *11* (34), 31467-31476.

24.     Wood, K. N.; Kazyak, E.; Chadwick, A. F.; Chen, K.-H.; Zhang, J.-G.; Thornton, K.; Dasgupta, N. P., Dendrites and pits: Untangling the complex behavior of lithium metal anodes through operando video microscopy. *ACS central science* **2016,** *2* (11), 790-801.

25.     Selis, L. A.; Seminario, J. M., Dendrite formation in Li-metal anodes: an atomistic molecular dynamics study. *RSC Advances* **2019,** *9* (48), 27835-27848.

26.     Guo, Y.; Li, H.; Zhai, T., Reviving lithium-metal anodes for next-generation high-energy batteries. *Advanced Materials* **2017,** *29* (29), 1700007.

27.     Frisch, M. J.; Trucks, G. W.; Schlegel, H. B.; Scuseria, G. E.; Robb, M. A.; Cheeseman, J. R.; Scalmani, G.; Barone, V.; Petersson, G. A.; Nakatsuji, H.; Li, X.; Caricato, M.; Marenich, A. V.; Bloino, J.; Janesko, B. G.; Gomperts, R.; Mennucci, B.; Hratchian, H. P.; Ortiz, J. V.; Izmaylov, A. F.; Sonnenberg, J. L.; Williams; Ding, F.; Lipparini, F.; Egidi, F.; Goings, J.; Peng, B.; Petrone, A.; Henderson, T.; Ranasinghe, D.; Zakrzewski, V. G.; Gao, J.; Rega, N.; Zheng, G.; Liang, W.; Hada, M.; Ehara, M.; Toyota, K.; Fukuda, R.; Hasegawa, J.; Ishida, M.; Nakajima, T.; Honda, Y.; Kitao, O.; Nakai, H.; Vreven, T.; Throssell, K.; Montgomery Jr., J. A.; Peralta, J. E.; Ogliaro, F.; Bearpark, M. J.; Heyd, J. J.; Brothers, E. N.; Kudin, K. N.; Staroverov, V. N.; Keith, T. A.; Kobayashi, R.; Normand, J.; Raghavachari, K.; Rendell, A. P.; Burant, J. C.; Iyengar, S. S.; Tomasi, J.; Cossi, M.; Millam, J. M.; Klene, M.; Adamo, C.; Cammi, R.; Ochterski, J. W.; Martin, R. L.; Morokuma, K.; Farkas, O.; Foresman, J. B.; Fox, D. J. *Gaussian 16 Rev. C.01*, Wallingford, CT, 2016.

28.     GaussView, V., Dennington, Roy; Keith, Todd A.; Millam, John M. Semichem Inc., Shawnee Mission, KS, 2016.

29.     Becke, A., Density-functional thermochemistry: The role of extract exchange. *J Chem Phys* **1993,** *98* (5), 648-5.

30.     Camacho-Forero, L. E.; Smith, T. W.; Bertolini, S.; Balbuena, P. B., Reactivity at the lithium–metal anode surface of lithium–sulfur batteries. *The Journal of Physical Chemistry C* **2015,** *119* (48), 26828-26839.

31.     Kendall, R. A.; Dunning Jr, T. H.; Harrison, R. J., Electron affinities of the first-row atoms revisited. Systematic basis sets and wave functions. *The Journal of chemical physics* **1992,** *96* (9), 6796-6806.

32.     Petersson, a.; Bennett, A.; Tensfeldt, T. G.; Al-Laham, M. A.; Shirley, W. A.; Mantzaris, J., A complete basis set model chemistry. I. The total energies of closed-shell atoms and hydrides of the first-row elements. *The Journal of chemical physics* **1988,** *89* (4), 2193-2218.

33.     Petersson, G.; Al-Laham, M. A., A complete basis set model chemistry. II. Open-shell systems and the total energies of the first-row atoms. *The Journal of chemical physics* **1991,** *94* (9), 6081-6090.

34.     Tomasi, J.; Mennucci, B.; Cammi, R., Quantum mechanical continuum solvation models. *Chemical reviews* **2005,** *105* (8), 2999-3094.

35.     Pascual-ahuir, J.-L.; Silla, E.; Tunon, I., GEPOL: An improved description of molecular surfaces. III. A new algorithm for the computation of a solvent-excluding surface. *Journal of Computational Chemistry* **1994,** *15* (10), 1127-1138.

36.     MATLAB 2018a, T. M., Inc., Natick, Massachusetts, United States.

37.     Hu, H.-S.; Zhao, Y.-F.; Hammond, J. R.; Bylaska, E. J.; Aprà, E.; van Dam, H. J.; Li, J.; Govind, N.; Kowalski, K., Theoretical studies of the global minima and polarizabilities of small lithium clusters. *Chemical Physics Letters* **2016,** *644*, 235-242.

38.     Terrabuio, L. A.; Teodoro, T. Q.; Rachid, M. G.; Haiduke, R. L., Systematic theoretical study of non-nuclear electron density maxima in some diatomic molecules. *The Journal of Physical Chemistry A* **2013,** *117* (40), 10489-10496.

39.     Wu, L. C.; Jones, C.; Stasch, A.; Platts, J. A.; Overgaard, J., Non-Nuclear Attractor in a Molecular Compound under External Pressure. *European Journal of Inorganic Chemistry* **2014,** *2014* (32), 5536-5540.

40.     Jensen, F., *Introduction to computational chemistry*. John wiley & sons: 2017.

41.     Hu, H.; Lu, Z.; Yang, W., Fitting molecular electrostatic potentials from quantum mechanical calculations. *Journal of chemical theory and computation* **2007,** *3* (3), 1004-1013.

42.     Cioslowski, J., A new population analysis based on atomic polar tensors. *Journal of the American Chemical Society* **1989,** *111* (22), 8333-8336.

43.     Peled, E.; Menkin, S., Review-SEI: Past, Present, and Future. *J. Electrochem. Soc.* **2017,** *164* (7), A1703-A1719.

44.      Liu, S.;  Deng, L.;  Guo, W.;  Zhang, C.;  Liu, X.; Luo, J., Bulk Nanostructured Materials Design for Fracture-Resistant Lithium Metal Anodes. *Advanced Materials* **2019,** *31* (15), 1807585.

Table of Content Figure
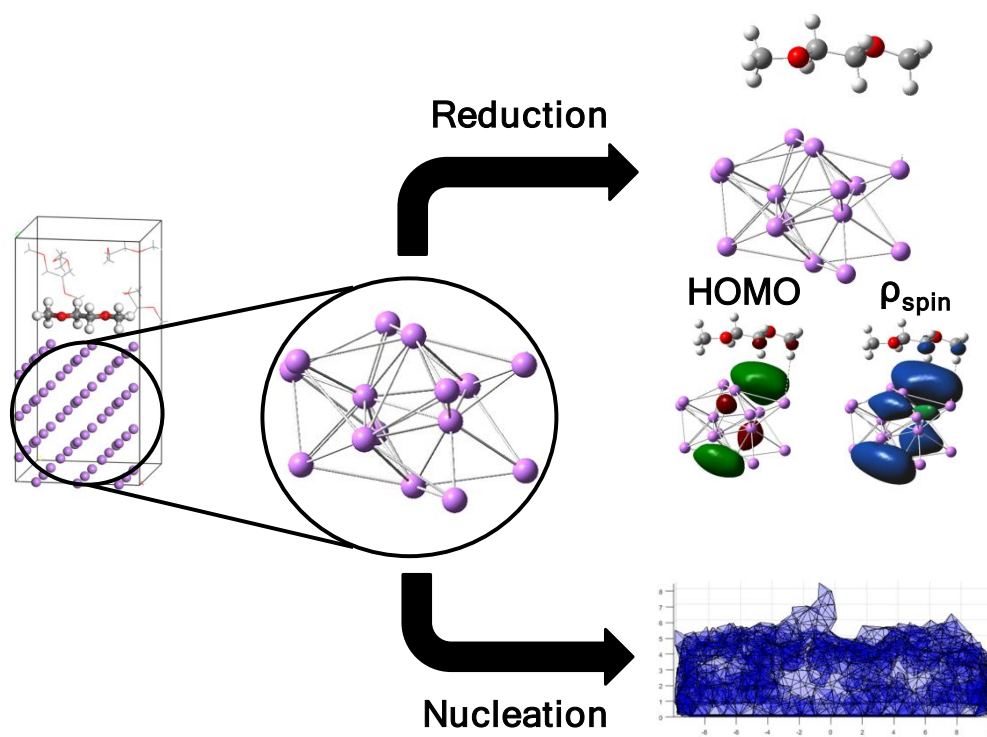


A simple approach based on first principles leads to investigate the origins of dendritic growth